





Article

Modal, Structural, and Comfort Analyses for Improving Customized Bicycles for Recreational Ridings of People with Disabilities

Andrey Maciel Araújo da Silva ¹, Sérgio de Souza Custódio Filho ², Leonardo Dantas Rodrigues ¹, Fábio Antônio do Nascimento Setúbal ¹, Sérgio Aruana Elarrat Canto ¹, Girlan Lucas da Costa Oliveira ¹, Ana Lúcia Nascimento Moraes dos Santos ¹, Wellington Lima Botelho ¹ and Alexandre Luiz Amarante Mesquita ^{1,*}

¹ Mechanical Engineering Faculty, Federal University of Pará, Belém 66075-110, Brazil; andreymaciel468@gmail.com (A.M.A.d.S.); leodr@ufpa.br (L.D.R.); fabioans@ufpa.br (F.A.d.N.S.); aruana@ufpa.br (S.A.E.C.); girlanlucas0@gmail.com (G.L.d.C.O.); analidia97@live.com (A.L.N.M.d.S.); wellingtonbotelhojr07@gmail.com (W.L.B.)

² Marabá Industrial Campus, Federal Institute of Pará, Marabá 68740-970, Brazil; sergio.custodio@ifpa.edu.br

* Correspondence: alexmesq@ufpa.br

Abstract: Leisure activities are known to be especially important for the health of people with disabilities. In Belém, PA, an Amazonian city in Brazil, a non-profitable organization has promoted leisure ridings in bicycles for those people in Utinga State Park, a large green area for physical and leisure activities. The handcrafted bikes have a sidecar attached for users with disabilities which are ridden by trained volunteers. Since such bikes have been empirically manufactured, they require some minor improvements in safety, comfort, and handling, and verification of structural strength. Therefore, ergonomic, modal, and forced vibration analyses assessed the user's comfort and safety and a structural analysis with the use of strain gauges evaluated the bicycle's structural strength. Initially, a numerical modal analysis was performed using the finite element method, and the modal model obtained was validated by an experimental modal analysis employing shaker excitation. ISO-2631-based evaluations of forced vibration and human body comfort were conducted regarding whole-body vibration in vehicles and mechanical equipment. Vibration measurements at the position of the rider and sidecar occupant were obtained during rides on the bicycle and, according to the results, in general, when subjected to loads, the bicycle showed low stress levels far from the yield stress of the material, promoting an excellent safety factor in relation to its structural integrity. The modal, comfort, and forced vibration analyses revealed a mode of vibration in the sidecar that caused discomfort to the back of the users. Ergonomics analysis pointed out changes in the handlebars, the bicycle seat, the coupling between the sidecar and the bike, and the dimensions of the sidecar will provide greater comfort and safety. This paper presents and discusses the proposed modifications to both bicycle and sidecar.

Keywords: adapted bicycle; vibration; modal analysis; structural integrity; ergonomics; people with disabilities



Citation: Silva, A.M.A.d.; Custódio Filho, S.d.S.; Rodrigues, L.D.; Setúbal, F.A.d.N.; Canto, S.A.E.; Oliveira, G.L.d.C.; Santos, A.L.N.M.d.; Botelho, W.L.; Mesquita, A.L.A. Modal, Structural, and Comfort Analyses for Improving Customized Bicycles for Recreational Ridings of People with Disabilities. *Vibration* **2024**, *7*, 687–704. <https://doi.org/10.3390/vibration7030036>

Academic Editor: Xavier Chimentin

Received: 29 April 2024

Revised: 23 June 2024

Accepted: 1 July 2024

Published: 4 July 2024



Copyright: © 2024 by the authors. Licensee MDPI, Basel, Switzerland. This article is an open access article distributed under the terms and conditions of the Creative Commons Attribution (CC BY) license (<https://creativecommons.org/licenses/by/4.0/>).

1. Introduction

The Brazilian population aged 65 and over accounted for 7.7% of the population in 2012, rising to 10.5% of the total population in 2022 [1]. Moreover, Brazilian life expectancy has already surpassed 73 years and is expected to reach 81 years by 2050 [2], which has led to an increasing number of elderly people. Problems arise with population aging, mainly concerning the health and well-being of the elderly. Therefore, public and private organizations have sought actions that provide well-being not only to the elderly but also to physically and visually impaired individuals through leisure activities [3–5]. Cycling, one of

such activities, offers many experiences that contribute to the well-being of individuals [6] facilitating the socialization of disabled individuals and reducing social exclusion [7]. In Brazil, examples of those inclusive actions include Bike Without Borders and Bike for All Projects [8]. The former, undertaken in Recife and in Rio de Janeiro, encourages disabled and elderly people to ride their bikes in pleasant places, close to nature, whereas the Bike for All Project of the Brazilian non-governmental organization (NGO) “Embrião” (Embryo, in English), from Alvorada city, in Rio Grande do Sul state, has developed adapted bicycles for visually impaired riders. Due to its success, it was replicated in Aracaju city (Sergipe State), in 2013. In Belém, PA, located in the north of Brazil, NGO “Ponto de Apoio” (Support Point, in English) promotes free rides on adapted bicycles for people with disabilities and the elderly in Utinga State Park. The bicycles are hand-made in an empirical way; they are functional and have met the NGO’s objectives. However, complaints from users—both volunteer monitors (who ride the bicycles) and project clients (people with disabilities)—regard the comfort of the rides.

Discomfort on bicycles has been the subject of several studies. Groenendijk et al. [9] claimed more than a million Dutch cyclists (approximately 36% men and 42% women, totaling a sample of 900 people) suffered from pain or discomfort in the body caused by cycling, and Christiaans and Bremner [10] reviewed several studies on general cyclist comfort and bicycle ergonomics. Hayot et al. [11] demonstrated how a cyclist’s posture can lead to physical injuries. Ayachi et al. [12] described the determining factors that contribute to comfort during cycling, identifying situations in which comfort is relevant and addressing how vibrations play a role in comfort assessments. Their research was corroborated by Gao et al. [13], who pointed out that vibration is perceived by cyclists as one of the most important indicators of cycling comfort.

The bicycles of the NGO “Ponto de Apoio” mentioned in the previous paragraph consist of bicycles made empirically, probably without technical rigor. The empirical approach generally emphasizes practical experience and the learning acquired through it, rather than strictly following scientific methods or pre-established techniques. Therefore, a project involving NGO “Ponto de Apoio”, professors, and students from the Federal University of Pará (Brazil) was developed towards improving drivability, ergonomics, and comfort, as well as enhancing the technical rigor in the manufacture of bicycles used by the aforementioned NGO. This paper discusses the results from improvements in those bicycles through numerical and experimental modal analyses, a comfort analysis involving whole-body vibration that checked the discomfort of users, and a structural analysis that examined the strength of the bicycle to operational forces. The following sections detail the numerical and experimental analyses, discuss the results, and present the modifications suggested for users’ comfort.

2. Methods

The NGO “Ponto de Apoio” has several bicycles for rides in Utinga Park (Figure 1), among which the users’ favorite one was chosen as a prototype for the improvement analyses. The custom bicycle (Figure 2) was handcrafted from steel tubes and has a sidecar attached to its side. It was built exclusively for the leisure activities of the “Ponto de Apoio” project and has no document with specifications such as characteristics and dimensions. Therefore, a numerical and experimental modal analysis, a structural strength analysis, an ergonomic analysis, and a whole-body vibration analysis were performed towards a complete diagnosis of the bicycle regarding safety, comfort, drivability, and resistance. The following sections describe the procedures of the analyses.



Figure 1. Bicycle from “Ponto de Apoio” project.



Figure 2. Images of the analyzed bicycle.

2.1. Modal Analysis

2.1.1. Numerical Modal Analysis by Finite Elements

A numerical modal analysis performed according to the finite element method examined the dynamic properties of the bicycle, which included characterization of its vibration modes. This numerical modal model was validated by an experimental modal analysis in the laboratory. In what follows is a description of the numerical modal analysis.

Initially, the modeling of the bicycle required measurements of the dimensions of both the bicycle and the sidecar and the diameter and thickness of each tube of the bicycle. FreeCAD 0.20.1 was the software chosen for the modeling. Figure 3 shows the result of the geometric model.

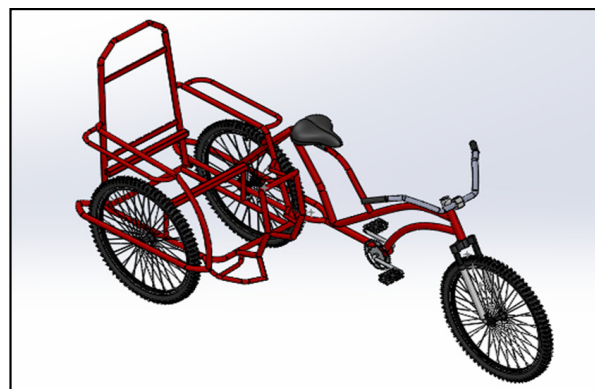


Figure 3. Geometric model of the bicycle in FreeCAD 0.20.1.

The geometric model was exported to Ansys version 11 finite element software for the pre-processing phase, in which the physical properties of the bicycle material, boundary conditions, element type, and mesh of the model were defined. The boundary conditions consist of elastic supports, which represent the flexibility of the tires. The elastic supports were placed in the centers of the wheel fixing structures, as shown in Figure 4. The physical properties used for the steel were a specific mass of 7800 kg/m^3 , a Young's modulus of 207 GPa , a Poisson's ratio of 0.3 , a shear modulus of 79.61 GPa , and a yield strength of 250 MPa . The panels present in the sidecar are made of plywood, having low stiffness and mass, which is why they were not considered in the modal analysis.

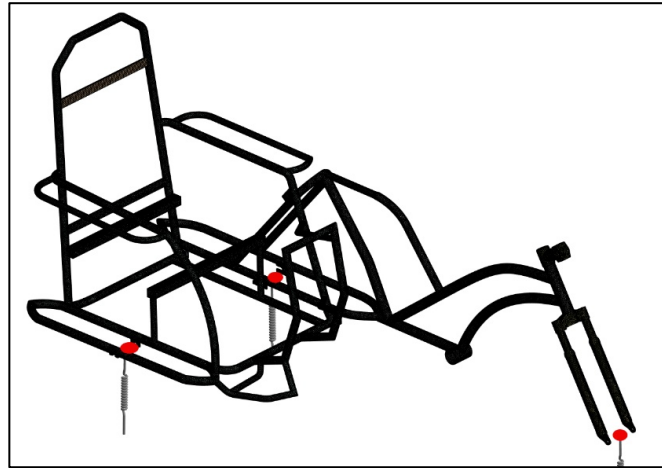


Figure 4. Finite element model of the bicycle and elastic supports (on red dots).

The mesh used in the model was defined after a convergence analysis based on the natural frequency results of the bicycle. Figure 5 displays the convergence analysis with the first four natural frequencies found as a function of the number of nodes of the mesh. The final mesh, composed predominantly of 4 mm tetrahedral elements, was constituted with $1,455,118$ nodes and $714,374$ elements.

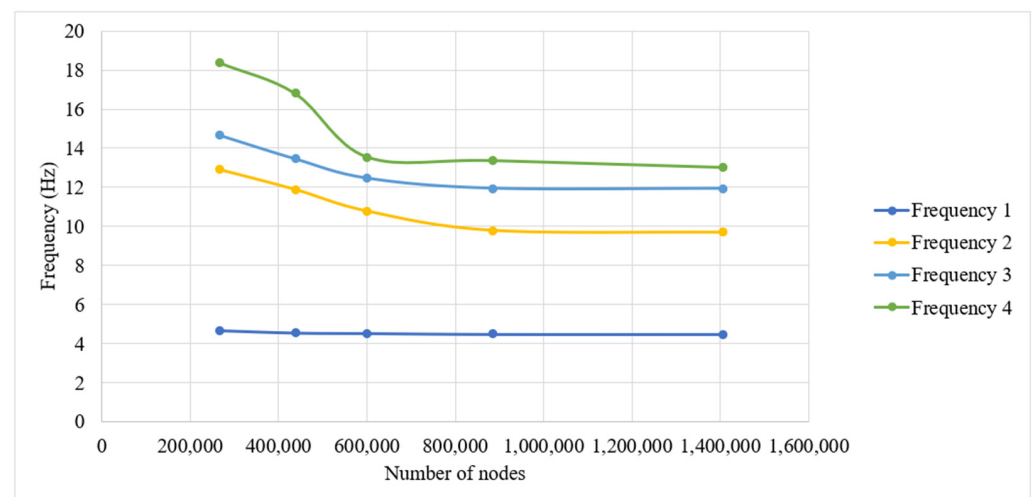


Figure 5. Mesh convergence analysis.

2.1.2. Experimental Modal Analysis

The frequency response functions (FRFs) of the bicycle were measured, from which the natural frequencies were obtained [14–16]. During the modal test, the bicycle was excited by a shaker, and an accelerometer measured the responses (Figure 6). The force and acceleration signals were sent to a signal analyzer for the FRFs processing (Figure 7). To

validate the numerical vibration modes, only the experimental natural frequencies were determined (modal shapes were not measured).



Figure 6. Shaker (left) and details of force and vibration transducers (right).



Figure 7. Signal analyzer.

2.2. Structural Integrity Analysis

Structural integrity analysis deals with the ability of a structure to support loads and thus prevent damage. A numerical structural integrity analysis using the finite element method was conducted for the adapted bicycle, and the results were validated experimentally by extensometry in the laboratory.

The same geometry and boundary conditions used in the modal analysis described in Section 2.1.1 were used for the numerical structural analysis. A force applied in the region corresponding to the saddle of the bike simulated the loading, and the mesh was refined in areas of higher stress concentration, such as welded joints. Figure 8 shows details of the loading (masses of set and cyclist and passenger mass), the elastic supports, and the final mesh.

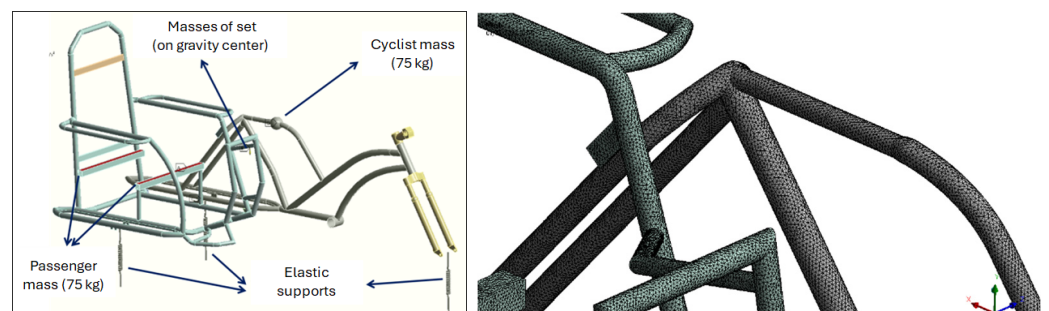


Figure 8. Load applied and elastic supports (left) and final mesh (right).

Extensometry is an experimental technique that measures the surface strains of a solid subjected to external forces [17]. Strain gauges (Figure 9) are bonded on the surface of a part that measures strain levels upon the application of a load. The technique is widely used for

verifications of stress levels of a structure—in our case, the bicycle and sidecar structures. The numerical model was validated by extensometry in a static analysis, and variations in strains under dynamic efforts in the bicycle ride were evaluated in different soil types for analyses of impact effects and fatigue [18–20].

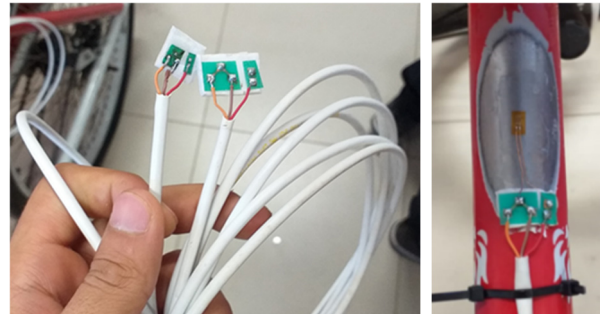


Figure 9. Strain gauges and cables (left); strain gauge fixed to the bike frame (right).

2.3. Ergonomic and Whole-Body Vibration Analyses

The comfort analysis involved investigating users' complaints, analyzing the posture of the driver, measuring and analyzing the vibration transmitted to users (driver and passenger), and analyzing the gear ratio of the bicycle to reduce the driver's efforts.

Single-speed gear ratio, passenger's position on the driver's side, and the red color of the bicycle were premises of the project (required by the Ponto de Apoio Group), i.e., they could not be changed.

The posture of the cyclist is crucial for comfort analysis for preventing injuries and improving his/her performance [11]. The ergonomic analysis of the project's bicycle was conducted according to two approaches, i.e., one focusing on the cyclist's body measurement and assisting in the definition of the appropriate length and height for the different components of the bicycle [21] and another focusing on the posture of the cyclist during the activity, defining angles for the different articulations of the body [22].

The evaluation of vibration and human body comfort was based on ISO 2631-1 [23], which addresses whole-body vibrations in vehicles and mechanical equipment. ISO 8041 [24] was also adopted since it establishes vibration measurement procedures, focusing on the filtering and weighting of the signal, and adapting it to the sensitivity of the human body. The whole-body vibration assessment involved measurements of vibrations to which both rider and sidecar occupant were exposed during the rides. In such rides, the bicycle was taken to the Federal University of Pará parking lot (Figure 10a), and an accelerometer was positioned on the saddle (Figure 10b), the passenger seat (Figure 10c), and the backrest (Figure 10d). Rides were performed on an asphalt-lined track and on a cobblestone track to simulate the walking conditions of Utinga Park.



Figure 10. Measurements of whole-body vibrations: (a) measurement during bike rides; (b) sensor placed on saddle; (c) sensor placed on passenger seat; (d) sensor placed on sidecar backrest.

An important factor for the optimization of the gear ratio of the bike is the analysis of its intention of use. The functionality of the bicycle under analysis is related to rides at moderate speeds. The gear ratio used was heavy, with 36 front gear (chainring) teeth and 13 rear gear (cog) teeth (2.77 gear ratio), resulting in a considerable effort applied by the cyclist to the pedals to make the bicycle move, especially at the beginning of its movement. The analysis, which related effort to the gear ratio, defined the new gear ratio, presented in Section 3.

3. Results and Discussion

3.1. Modal Analysis Results

In the numerical modal analysis, the first four vibration modes were calculated. Figures 11 and 12 show the first four vibration modes obtained for the bicycle with the sidecar. In the first mode, we can see a high vibration along the back of the sidecar.

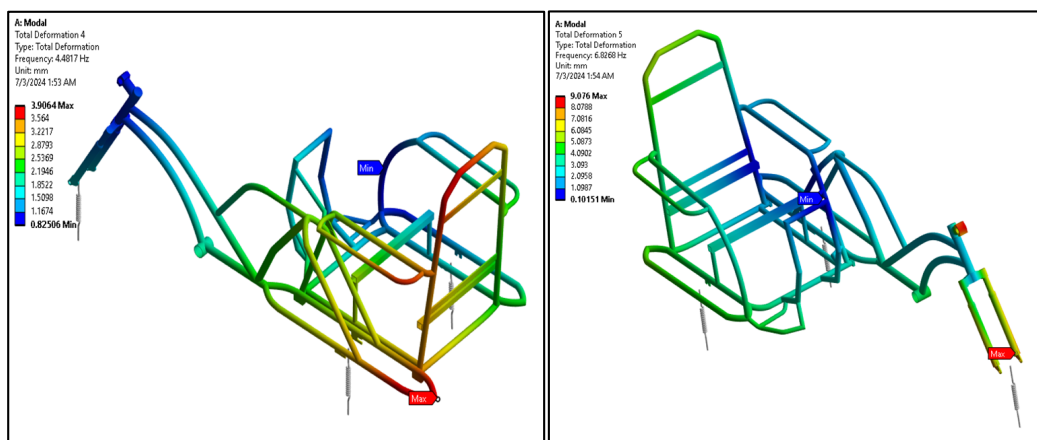


Figure 11. First numerical mode: 4.48 Hz (left); second numerical mode: 6.82 Hz (right).

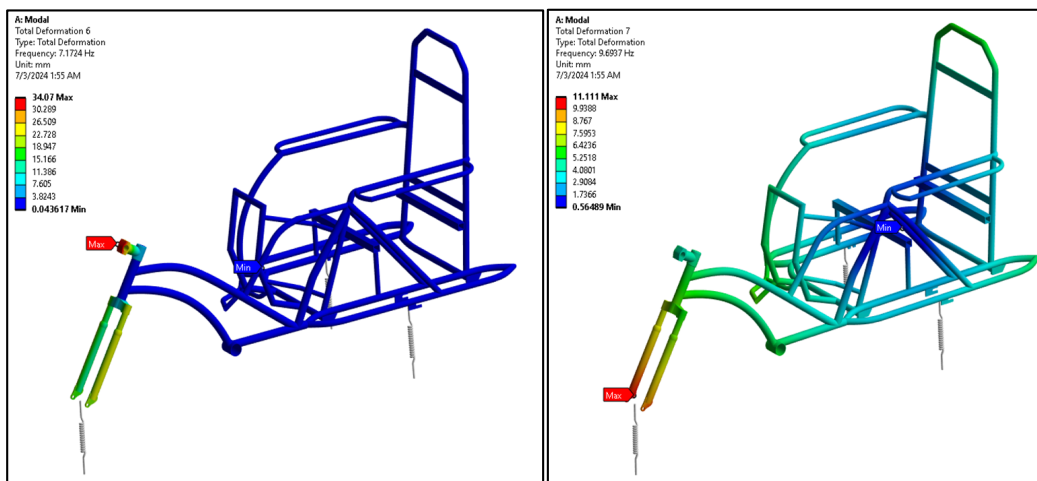


Figure 12. Third numerical mode: 7.17 Hz (left); fourth numerical mode: 9.69 Hz (right).

Experimentally, thirty-two FRFs were measured for the obtaining of the modal parameters. Concerning the modal shapes, they are very difficult to obtain experimentally because they involve all three directions, which would require excitation and response in the different directions. For this reason, in this study, the numerical model was only validated for the natural frequencies. Figure 13 illustrates one of the FRFs obtained in the experimental stage and the respective coherence function, showing the quality of the measured FRF. The FRF shown in Figure 13 shows a peak at the first natural frequency, while other FRFs provided information for identifying the other modes. The FRFs obtained

were submitted to TestLab Rev 4B modal parameter identification software for the determination of the experimental vibration modes of the bicycle. The numerical and experimental natural frequency values are shown in Table 1, according to which the results are in good agreement, validating the numerical model.

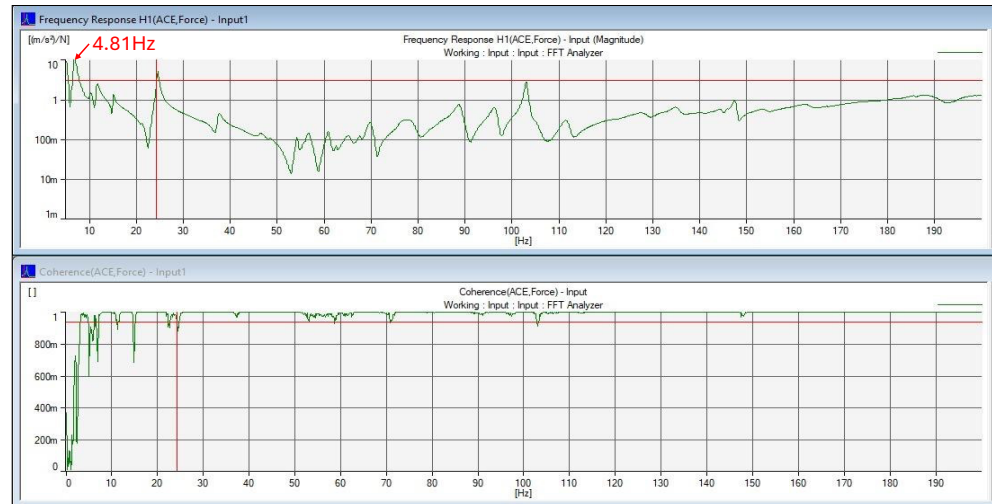


Figure 13. Frequency-response function (FRF) (**upper plot**) and its coherence function (**bottom plot**). The intersection of the horizontal and vertical red lines indicates the position of the cursor on the plots.

Table 1. Experimental and numerical natural frequencies.

Mode	Experimental Natural Frequency	Numerical Natural Frequency	Error %
1st	4.81 Hz	4.48 Hz	6.86
2nd	6.32 Hz	6.82 Hz	7.91
3rd	7.58 Hz	7.17 Hz	5.41
4th	9.38 Hz	9.69 Hz	3.30

The first vibration mode is probably the most easily achievable and corresponds to the vibration in the sidecar’s backrest, corroborating users’ reports of certain discomfort in this region. The first optimization proposed is the addition of an extra bar at the rear of the sidecar, stiffening the structure and tending to increase its natural frequencies. The second optimization is the addition of shock absorbers in the connection of the sidecar to the main frame and the wheel, increasing the damping of the set. More details of these changes are presented in Section 3.4.

A numerical modal analysis of the optimized design (which will be shown in detail in Section 3.4) was also performed. After a convergence test, the elements were configured to size up to 4 mm, generating a mesh of 900,193 elements and 1,682,508 nodes. Similar to tires, the shock absorbers were modeled as elastic supports with a stiffness coefficient of 100 N/mm (average value found in commercially available models). In the analysis, the mesh is shown in Figure 14.

The damping effect caused by the shock absorbers was not evaluated in this work since numerical modal analyses do not consider nonlinearities. This effect could be the subject of future studies through more elaborate dynamic analyses through harmonic or transient analyses. As in the analysis of the original design, the first four vibration modes were calculated and are presented in Figures 15 and 16, and the natural frequencies are shown in Table 2. It is observed that natural frequencies have increased, given the stiffening of the structure, which tends to improve user comfort. The frequency of the first mode has been increased, and the high vibration along the side has disappeared, remaining only in the upper bar, which can be solved by padding.

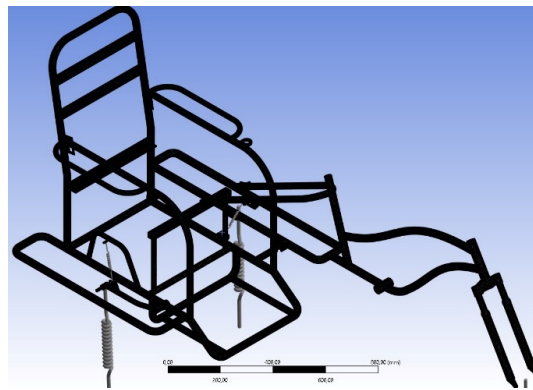


Figure 14. Finite element model of the optimized design.

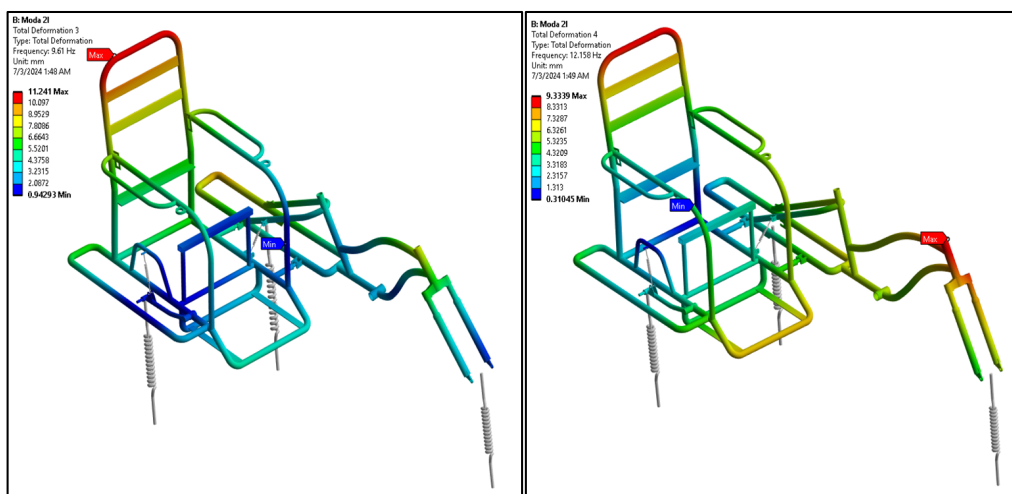


Figure 15. First numerical mode: 9.61 Hz (left); second numerical mode: 12.15 Hz (right).

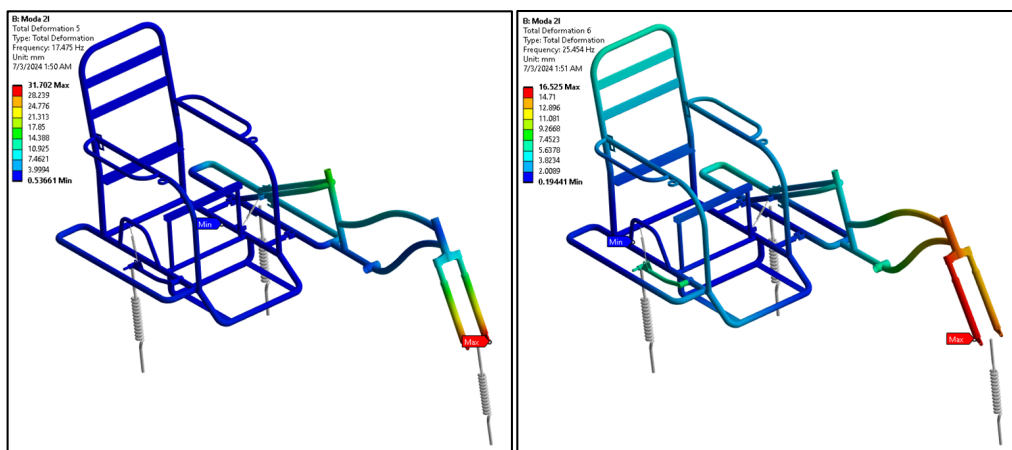


Figure 16. Third numerical mode: 17.47 Hz (left); fourth numerical mode: 25.45 Hz (right).

Table 2. Natural frequencies for the optimized design.

Mode	Numerical Natural Frequency
1st	9.61 Hz
2nd	12.15 Hz
3rd	17.47 Hz
4th	25.45 Hz

3.2. Structural Integrity Analysis Results

The numerical model was also validated from the strain results of the static analysis with strain gauges (Figure 17) through a comparison of the strain results from the experimental test with those of the numerical simulation (Table 3). In the experiment to validate the numerical model, the load used in the experiment was the weight of a 75 kg person sitting on the saddle without supporting either their feet or hands anywhere on the bicycle.



Figure 17. Use of strain gauges for numerical model validation (left) and their positions on bicycle (right).

Table 3. Strain values—experimental and numerical model.

Strain Gauge	Strain—Experimental Testing ($\mu\text{m/m}$)	Strain—Numerical Simulation ($\mu\text{m/m}$)	Error
1	52.5	52.6	−0.2%
2	−8.3	−8.5	−2.4%
3	−43.4	−38.2	−12.0%

Note for position “1” and “2”, the percentages of errors were minimal, whereas for position “3”, the percentage was higher but acceptable. The results enabled a full correlation of the numerical model with the experimental one, validating the numerical model. In the numerical model, the positions with the highest equivalent stresses along the structure were selected, as shown in Figure 18. The points with the highest stresses provided by the numerical model are not the same as the points where the strain gauges are positioned (although some are close).

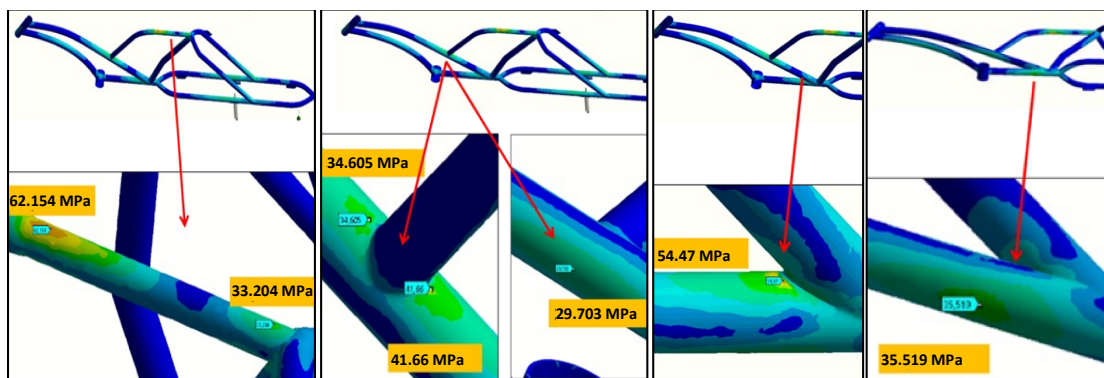


Figure 18. Points with highest equivalent stress values.

In general, the structure showed very low equivalent stresses, with 62.154 MPa as the maximum, resulting in a safety factor of approximately four. Few regions of high stresses were observed due to localized effects of stress concentrations or contact; however, even in such areas, the equivalent stresses were far from the yield stress of the material, which, in this case, was 250 MPa (structural steel).

Figure 19 displays values for the safety factor (SF) on the bicycle, calculated by the von Mises method, for which the minimum acceptable value is one. The minimum value obtained in the simulations was three in a few points. In most parts of the structure, safety factors are close to 15, indicating the bicycle is very safe for the static loads tested.

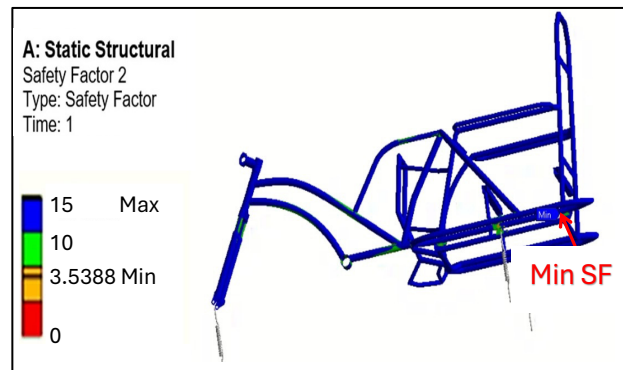


Figure 19. Gradient of SF values and different bicycle views.

The strain dynamic analysis involved a study of strains in the bicycle frame at the points examined in the static analysis. A methodology developed enabled the understanding of the influence of the type of soil on the dynamic behavior of the bicycle’s frame. According to the analysis of the strains of the three strain gauges (SGs) as a function of time (Figure 20), the fluctuations follow specific patterns at certain times since the bicycle was subjected to three different soils, called “A”, “B”, and “C”, thus generating different strain fluctuations in the selected regions. Table 4 shows the maximum, minimum, and variation strain values according to the soil on which the bicycle was ridden.

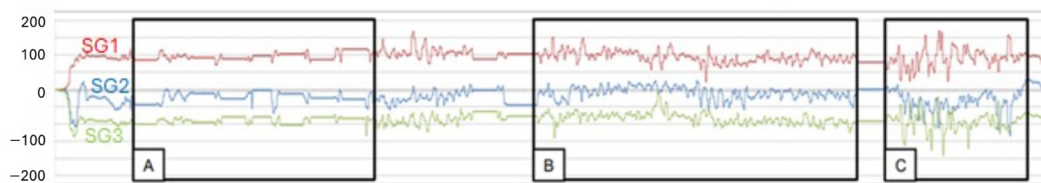


Figure 20. Strain variations (µm/m) as a function of time and soils (A–C).

Table 4. Maximum and minimum strain values and variation.

Strain Gauge	A			B			C		
	1	2	3	1	2	3	1	2	3
Maximum strain (µm/m)	118	−68	−133	150	−133	−140	170	−133	−190
Minimum strain (µm/m)	72	1	−73	23	−73	−9	24	13	−22
Variation (µm/m)	46	−69	−60	127	−87	−131	146	−146	−168

The bicycle showed fluctuation with higher values of strain in type “C” soil due to its irregularities, thus requiring greater efforts. Similarly, in type “A” soil, the bicycle showed lower deformation fluctuations since the soil does not have so many irregularities, requiring low effort. Finally, the strains of type “B” soil were smaller than those of “C” but

larger than the ones of “A”. For the three types of soil, the efforts generated by the dynamic strains were well below the yield strength of the material; moreover, the fatigue analysis pointed to a long enough life (over 5×10^5 cycles) due to the stress ranges obtained in the analyses.

3.3. Ergonomic and Whole-Body Vibration Analysis Results

Users reported some slight discomfort in both the passenger’s back in the sidecar and the driver’s due to their posture on the bicycle, excessive efforts by the driver at the beginning of the movement, discomfort caused by the handlebars, the sidecar being too close to the driver’s legs, and many sharp corners on the bike, among other types of discomforts. Such points indicated in the interviews were corroborated in an ergonomic evaluation of the cyclist’s posture with the bicycle stopped and in motion, the passengers’ and cyclists’ comfort during the ride, and the design of the bicycle. Figure 21 shows some results of the evaluation, such as the presence of sharp corners in the bicycle’s structure, the curved back of the rider, and the rider’s arms being too open. Some of the other factors identified in the interviews and checked in the ergonomic evaluation were the tendency of the bicycle to fall, the cyclist’s efforts when starting to pedal, the tendency of the bicycle to turn to one side (especially in curves), and discomfort in the rider’s back. All such points were considered for the final design of the optimized bicycle.

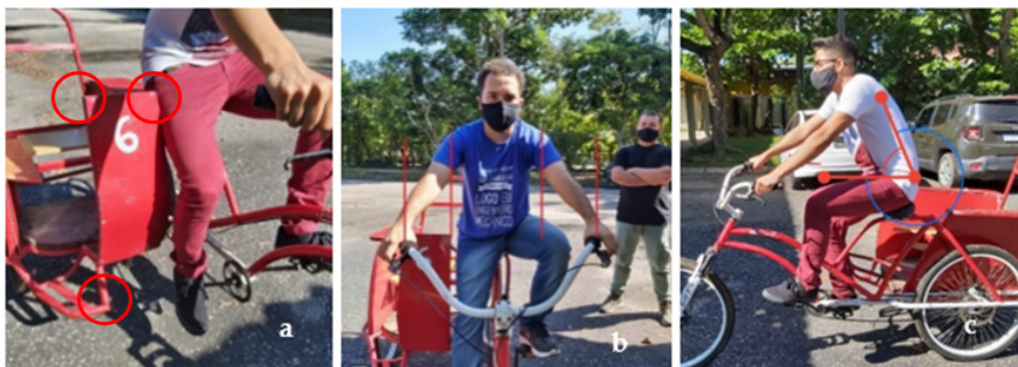


Figure 21. Ergonomic evaluation: (a) possible shocks due to sharp corners; (b) shoulder and wrists misaligned; (c) curved spine.

The evaluation of comfort from the vibration values obtained experimentally was based on ISO 2631-1 standard [23], which provides a range of acceleration amplitudes for the determination of the level of comfort on public transport, summarized in Table 5 in a color code.

Table 5. Levels of acceleration amplitude and comfort according to ISO 2631-1 [23].

Acceleration Amplitude	Level of Comfort
Less than 0.315 m/s^2	Not uncomfortable
Between 0.315 m/s^2 and 0.63 m/s^2	A little uncomfortable
Between 0.5 m/s^2 and 1 m/s^2	Fairly uncomfortable
Between 0.8 m/s^2 and 1.6 m/s^2	Uncomfortable
Between 1.25 m/s^2 and 2.5 m/s^2	Very uncomfortable
More than 2 m/s^2	Extremely uncomfortable

After the measurements, the vibration values were processed according to ISO 2631-1 [23] and ISO 8041 [24] (see Figure 22 for positions and ground types). These acceleration amplitudes were calculated with weights in the frequency domain according to the standard. The results showed that the vibration induced on users caused discomfort, as previously reported by them, demanding modifications in the bicycle design.

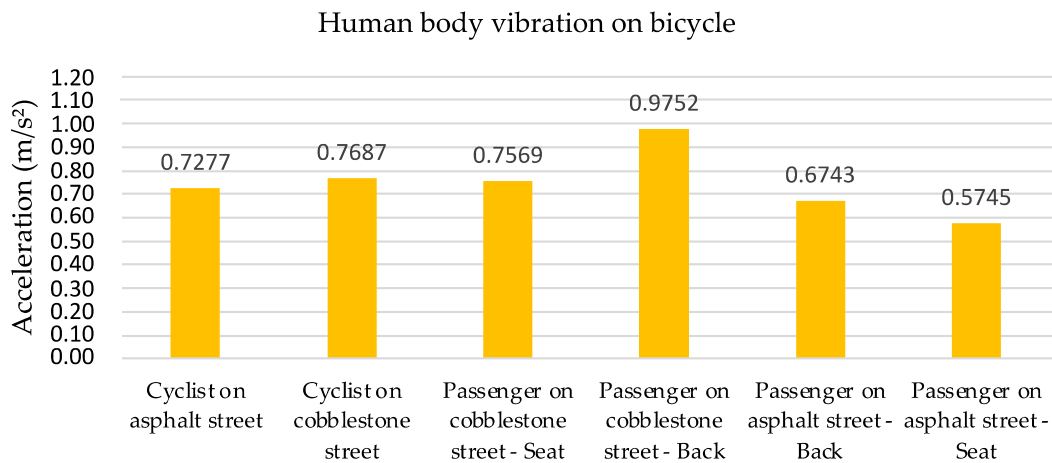


Figure 22. Comfort level according to ISO 2631-1 [23].

Regarding gear transmission, speed has a high gear ratio of $r = 2.77$. Table 6 shows different gear ratios correlated to the effort expended by the rider. The ideal ratios for rides at moderate speeds and with little rider effort are provided in green. The chainring with 36 teeth was kept, and the cog was changed to one with 24 teeth in this study. The ratio was also changed to $r = 1.50$.

Table 6. Pedaling effort level and speed ratio: high effort (orange), moderate effort (blue), low effort (green) [25].

Ring Cog	36	37	38	39	40	41	42	43	44	45	46	47	48	Ring Cog
13	2.77	2.85	2.92	3.00	3.08	3.15	3.23	3.31	3.38	3.46	3.54	3.62	3.69	13
14	2.57	2.64	2.71	2.79	2.86	2.93	3.00	3.07	3.14	3.21	3.29	3.36	3.43	14
15	2.40	2.47	2.53	2.60	2.67	2.73	2.80	2.87	2.93	3.00	3.07	3.13	3.20	15
16	2.25	2.31	2.38	2.44	2.50	2.56	2.63	2.69	2.75	2.81	2.88	2.94	3.00	16
17	2.12	2.18	2.24	2.29	2.35	2.41	2.47	2.53	2.59	2.65	2.71	2.76	2.82	17
18	2.00	2.06	2.11	2.17	2.22	2.28	2.33	2.39	2.44	2.50	2.56	2.61	2.67	18
19	1.89	1.95	2.00	2.05	2.11	2.16	2.21	2.26	2.32	2.37	2.42	2.47	2.53	19
20	1.80	1.85	1.90	1.95	2.00	2.05	2.10	2.15	2.20	2.25	2.30	2.35	2.40	20
21	1.71	1.76	1.81	1.86	1.90	1.95	2.00	2.05	2.10	2.14	2.19	2.24	2.29	21
22	1.64	1.68	1.73	1.77	1.82	1.86	1.91	1.95	2.00	2.05	2.09	2.14	2.18	22
23	1.57	1.61	1.65	1.70	1.74	1.78	1.83	1.87	1.91	1.96	2.00	2.04	2.09	23
24	1.50	1.54	1.58	1.63	1.67	1.71	1.75	1.79	1.83	1.88	1.92	1.96	2.00	24

3.4. Bicycle Improvements Suggested

A set of flaws in the current model of the customized bicycle was established according to the structural, modal, and ergonomic analyses. The bicycle presented problems such as vibration, excessive effort by the rider when pedaling, and inadequate dimensions of the frame and sidecar, leading to problems of comfort and ergonomics, among others. According to the diagnosis, a new bicycle model was designed in SolidWorks (Figure 23) with the necessary changes to solve the problems detected.

The design of the sidecar was based on Brazilian technical standard (NBR, acronym in Portuguese) 9050 [26], which is related to accessibility to buildings, furniture, spaces, and urban equipment and establishes reference dimensions for manual or motorized wheelchairs. Safety items such as a handhold bar and a seat belt (Figure 24a) were added to the new model. A damper was included to minimize impacts and vibrations in the sidecar (Figure 24b), and a bar on the sidecar backrest reinforced the frame and reduced the effects of vibration (Figure 24c).

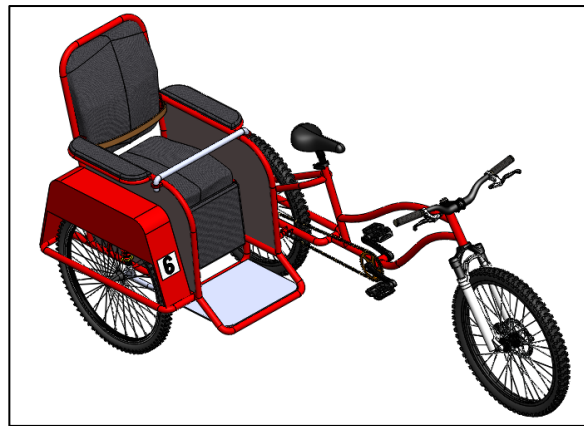


Figure 23. New model of customized bicycle.

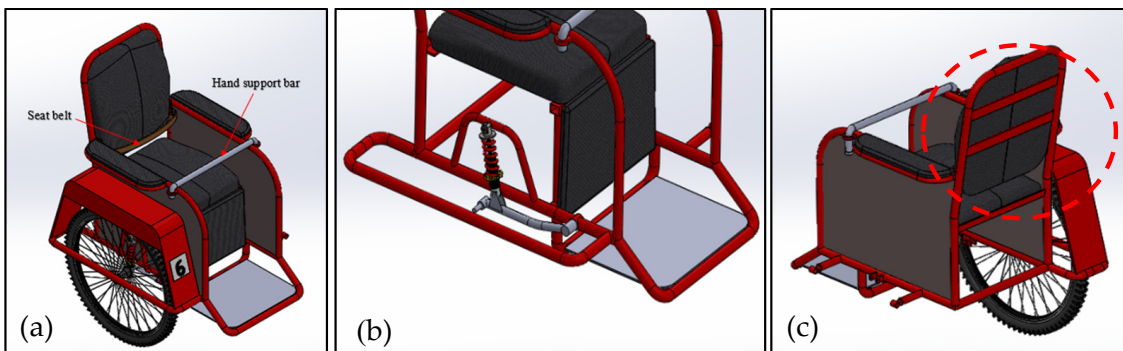


Figure 24. Modification details: (a) seat belt and handhold bar; (b) damper; (c) reinforcement bars on the sidecar back (highlighted in red dashed line).

The dimensions of the sidecar were different from the values established by the NBR 9050 standard [26]. The structure had excessively sharp corners, making it prone to accidents due to collisions with cyclists or sidecar passengers. Figure 25 shows the dimensions of the new sidecar and a comparison with the current model, respectively. Table 7 provides ideal values for the sidecar according to NBR 9050 [25] and the values adopted in the new sidecar.

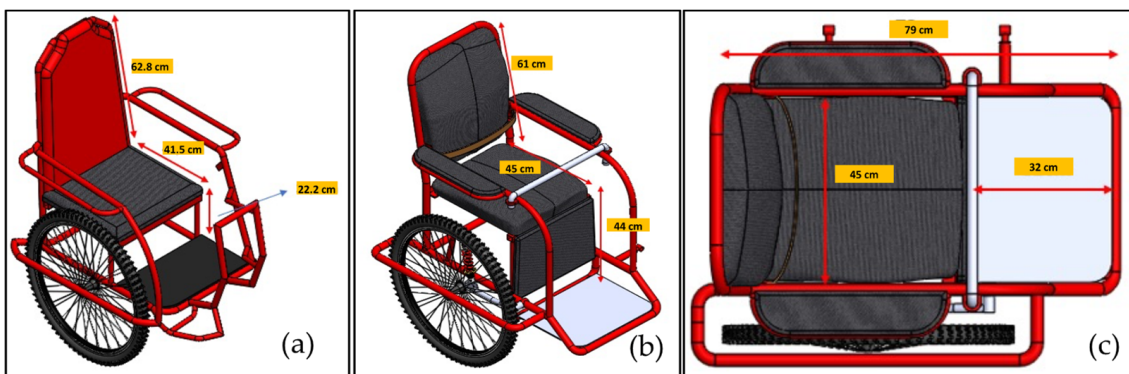
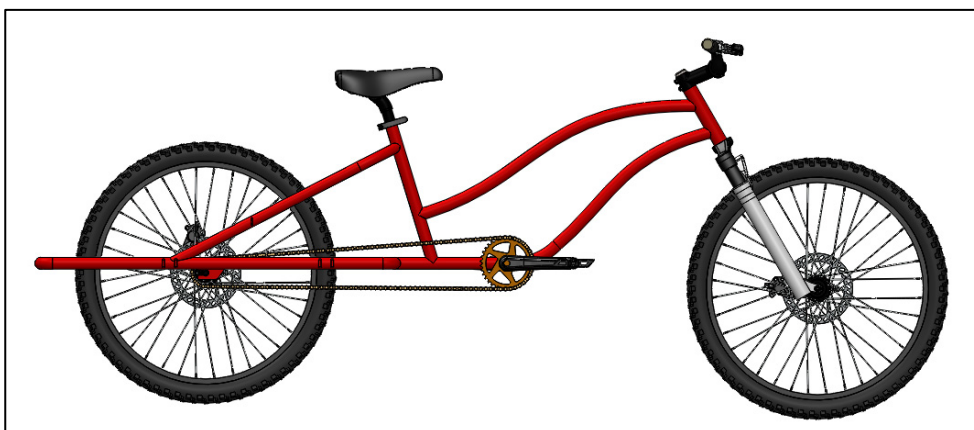


Figure 25. (a) Current model; (b) isometric view; and (c) top view of the new model.

Table 7. Ideal dimensions for sidecar and values adopted in the design.

Parameter	Value
Seat height between 40 and 45 cm	44 cm
Seat height between 40 and 45 cm	45 cm
Seat length between 42 and 45 cm	45 cm
Passenger backrest inclination between 100° and 105°	100°
Foot space between 30 and 40 cm	32 cm

The frame of the bicycle (Figure 26) was changed to a female pattern for better rider accessibility. The structural integrity analysis was again conducted and revealed a factor of safety similar to the one of the previous analyses. The bike was quite robust in both frame configurations, easily supporting the loads imposed during rides. A tube was included for adjusting the height of the saddle (Figure 27a) so that it could be used by people of different heights and provide the rider with the ideal posture. The handlebar model used in the bicycle was also changed (Figure 27b) to avoid collisions with the cyclist's legs and promote a correct alignment of the hands with the shoulders. Figure 27c displays the new chain drive system with a 1.50 transmission speed ratio.

**Figure 26.** New custom bike model.**Figure 27.** Bicycle details: (a) adjustable seat; (b) standardized handlebars; (c) new mechanical transmission.

A new rotating coupling system (Figure 28a) replaced the rigid coupling used in the current model and enabled an angular movement of the sidecar relative to the bicycle, improving drivability (the current bike tends to turn to the sidecar side). Finally, a shock absorber (Figure 28b) was inserted to prevent collisions between the sidecar and the bike. More details about rotating coupling and shock absorber are shown in Figure 29.

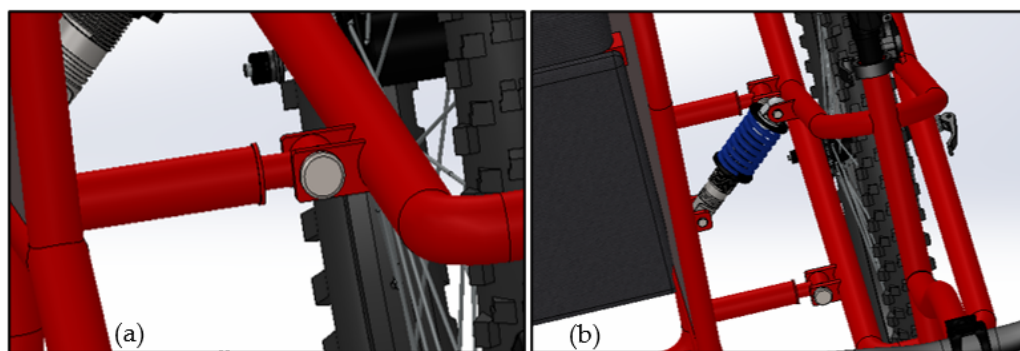


Figure 28. Connections between sidecar and bicycle. (a) rotating coupling; (b) shock absorber.

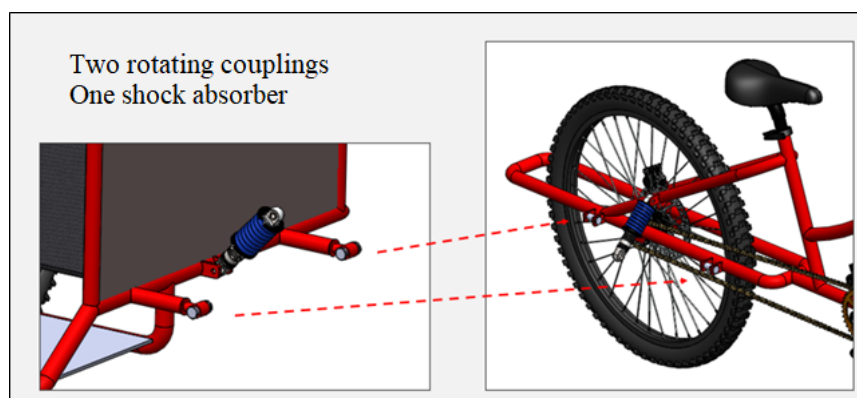


Figure 29. Details of connections between sidecar and bicycle.

4. Conclusions

This paper presented the results of a modal analysis, a structural integrity analysis, and a comfort analysis of an empirically manufactured bicycle adapted with a sidecar for leisure rides of people with disabilities in Utinga State Park in Belém, PA, northern Brazil. The analyses provided a better design towards greater comfort and safety to both the cyclist and the user with disabilities.

The general procedure was initially to obtain information on complaints from users of the customized bicycle (without the modifications) and then to carry out an ergonomic analysis based on national and international technical standards, a comfort analysis based on vibration measurements, a modal analysis to verify the occurrence of resonances, and an analysis of the structural strength of the adapted bicycle, since it was manufactured empirically.

The modal analysis revealed that the first mode of vibration, easily reachable, caused the sidecar backrest to vibrate with high amplitudes. The structural integrity analysis showed the bicycle is robust and easily supports the loads imposed during the rides. For the proposed design, the modal analysis showed an increase of approximately double the frequency value for this mode. The comfort analysis was conducted in three stages. The first, aiming at ergonomics, included an interview with users and checked the angulations of the cyclist proposed by the literature, whereas the second focused on forced vibrations in the human body and included whole-body vibration analyses according to international standards. The third and last step examined drivability towards reducing efforts during the ride.

The first stage of the comfort analysis indicated several modifications should be made to both sidecar and bicycle. Regarding the former, a readjustment of its dimensions, inclusion of a safety belt, a hand bar, and a vibration damper and reinforcement in the backrest with increased rigidity and damping for reductions in vibration were defined. Such necessary changes were identified in the modal and whole-body vibration analyses, as further reported. The frame configuration of the bicycle was modified to facilitate the

cyclist going up and down, and the handlebars and saddle were changed. The vibration levels in the second analysis, measured according to international standards, showed the bicycle caused discomfort, which was corroborated by interviews with users and by the modal analysis. The main discomfort was vibration in the sidecar, for which the insertion of a vibration damper for the tire and reinforcement in stiffness and damping in the sidecar's backrest was defined, as addressed elsewhere. The third step revealed the need for the insertion of a coupling for a smooth relative angular movement between the bicycle and the sidecar since the bicycle tended to turn to the sidecar side. Therefore, two rotating couplings and a shock damper were inserted between the sidecar and the bicycle. Finally, the bike's transmission ratio was changed to reduce the rider's efforts during rides.

The results of the analyses led to the elaboration of an optimized design of the bicycle with a sidecar aiming at both greater comfort and safety for the users, thus making the rides much safer and more enjoyable due to the contact with the Amazonian nature in Utinga State Park. Regarding the scalability of this procedure, the methodology applied can be replicated for different customized bicycles for disabled people.

Author Contributions: Conceptualization, A.L.A.M. and A.M.A.d.S.; methodology, L.D.R., S.d.S.C.F. and S.A.E.C.; software, S.d.S.C.F., F.A.d.N.S., W.L.B., G.L.d.C.O. and A.L.N.M.d.S.; investigation, A.M.A.d.S., W.L.B., G.L.d.C.O. and A.L.N.M.d.S.; writing—original draft preparation, A.L.A.M. and A.M.A.d.S.; writing—review and editing, A.L.A.M. and L.D.R. All authors have read and agreed to the published version of the manuscript.

Funding: This research received no external funding.

Data Availability Statement: The data are available from the corresponding author on reasonable request.

Acknowledgments: The authors acknowledge the NGO “Ponto de Apoio” and the Institutional Extension Scholarship Program (PIBEX) of the Federal University of Pará for their support.

Conflicts of Interest: The authors declare no conflicts of interest.

References

1. Instituto Brasileiro de Geografia e Estatística—IBGE. Pesquisa Nacional por Amostra de Domicílio Contínua—PNAD Contínua. “Características Gerais dos Domicílios e dos Moradores 2022”. 2023. Available online: <https://biblioteca.ibge.gov.br/index.php/biblioteca-catalogo?view=detalhes&id=2102004> (accessed on 10 April 2024).
2. Santos, P.; Marinho, A.; Mazo, G.; Hallal, P. Leisure Activities and Quality of Life of older Adults Participating in an Exercise Intervention in Florianópolis, Brazil. *Rev. Bras. Atividade Física Saúde* **2014**, *19*, 494–503. [[CrossRef](#)]
3. McConkey, R.; Pochstein, F.; Carlin, L.; Menke, S. Promoting the Social Inclusion of Players with Intellectual Disabilities: An Assessment Tool for Sport Coaches. *Sport Soc.* **2021**, *24*, 430–439. [[CrossRef](#)]
4. Choi, C.; Bum, C.H. Physical Leisure Activity and Work for Quality of Life in the Elderly. *J. Phys. Educ. Sport* **2019**, *2019*, 1230–1235.
5. Mori, G.; Silva, L.F. da Leisure in the Third Age: Human Development and Quality of Life. *Mot. Rev. Educ. Física* **2010**, *16*, 950–957. [[CrossRef](#)]
6. Aksöz, O.; Aşan, K. Bicycle Touring Experiences as a Social Inclusion Activity for Visually Disabled Individuals. *Tour. Hosp. Manag.* **2021**, *28*, 445–464.
7. Dunford, C.; Rathmell, S.R.; Bannigan, K. Learning to Ride a Bike: Developing a Therapeutic Intervention. *Children Young People & Families Occupational Therapy Journal* 2017. Available online: <http://bura.brunel.ac.uk/handle/2438/18165> (accessed on 10 April 2024).
8. Teixeira, K.S.; Alves, M.P. Pedal Pedagogy, Urban Tribes and Tribes and Practical Educational Policies: First Approaches. *Rev. Teias* **2021**, *22*, 353–369. [[CrossRef](#)]
9. Groenendijk, M.C.; Christiaans, H.; Van Hulten, C.M.J. Sitting Comfort on Bicycles. In *Contemporary Ergonomics*; CRC Press: Boca Raton, FL, USA, 2020; pp. 551–557.
10. Christiaans, H.H.C.M.; Bremner, A. Comfort on Bicycles and the Validity of a Commercial Bicycle Fitting System. *Appl. Ergon.* **1998**, *29*, 201–211. [[CrossRef](#)] [[PubMed](#)]
11. Hayot, C.; Decatoire, A.; Bernard, J.; Monnet, T.; Lacouture, P. Effects of ‘Posture Length’ on Joint Power in Cycling. *Procedia Eng.* **2012**, *34*, 212–217. [[CrossRef](#)]
12. Ayachi, F.S.; Dorey, J.; Guastavino, C. Identifying Factors of Bicycle Comfort: An Online Survey with Enthusiast Cyclists. *Appl. Ergon.* **2015**, *46*, 124–136. [[CrossRef](#)] [[PubMed](#)]

13. Gao, J.; Sha, A.; Huang, Y.; Hu, L.; Tong, Z.; Jiang, W. Evaluating the Cycling Comfort on Urban Roads Based on Cyclists' Perception of Vibration. *J. Clean. Prod.* **2018**, *192*, 531–541. [[CrossRef](#)]
14. Ewins, D.J. *Modal Testing: Theory, Practice and Application*; John Wiley & Sons: Hoboken, NJ, USA, 2009.
15. He, J.; Fu, Z.-F. (Eds.) *Modal Analysis*; Butterworth-Heinemann: Oxford, UK, 2001; pp. 1–11; ISBN 978-0-7506-5079-3.
16. Setúbal, F.A.d.N.; Custódio Filho, S.d.S.; Soeiro, N.S.; Mesquita, A.L.A.; Nunes, M.V.A. Force Identification from Vibration Data by Response Surface and Random Forest Regression Algorithms. *Energies* **2022**, *15*, 3786. [[CrossRef](#)]
17. Dally, J.W.; Riley, W.F. *Experimental Stress Analysis*, 3rd ed.; McGraw-Hill: New York, NY, USA, 1991.
18. Rodrigues, L.D.; Freire, J.L.; Vieira, R.D. Development and Experimental Evaluation of a New Technique for the Measurement of Residual Tensions. *Matéria* **2011**, *16*, 842–856. [[CrossRef](#)]
19. Tomaszewski, T. Fatigue Life Analysis of Steel Bicycle Frame According to ISO 4210. *Eng. Fail Anal.* **2021**, *122*, 105195. [[CrossRef](#)]
20. de Souza Custódio Filho, S.; Santana, H.M.; Vaz, J.R.P.; Rodrigues, L.D.; Mesquita, A.L.A. Fatigue Life Estimation of Hydrokinetic Turbine Blades. *J. Braz. Soc. Mech. Sci. Eng.* **2020**, *42*, 281. [[CrossRef](#)]
21. Grainger, K.; Dodson, Z.; Korff, T. Predicting Bicycle Setup for Children Based on Anthropometrics and Comfort. *Appl. Ergon.* **2017**, *59*, 449–459. [[CrossRef](#)] [[PubMed](#)]
22. Burt, P. *Bike Fit 2nd Edition: Optimise Your Bike Position for High Performance and Injury Avoidance*; Bloomsbury Publishing: London, UK, 2022.
23. *ISO 2631-1; Mechanical Vibration and Shock: Evaluation of Human Exposure to Whole-Body Vibration*. 2nd ed. International Organization for Standardization: Geneva, Switzerland, 1997; Volume 1.
24. *ISO 8041; Human Response to Vibration: Measuring Instrumentation*. International Organization for Standardization: Geneva, Switzerland, 2017; Volume 1.
25. Saad, A.H. Bicycle Gear Ratio Table | BikeCalc—Bikecalc.Com. Available online: <https://www.bikecalc.com/archives/gear-ratios.html> (accessed on 10 April 2024).
26. Associação Brasileira de Normas Técnicas. *NBR 9050—Acessibilidade a Edificações, Mobiliário, Espaços e Equipamentos Urbanos*, 4th ed.; ABNT: Rio de Janeiro, Brazil, 2020; Volume 1.

Disclaimer/Publisher's Note: The statements, opinions and data contained in all publications are solely those of the individual author(s) and contributor(s) and not of MDPI and/or the editor(s). MDPI and/or the editor(s) disclaim responsibility for any injury to people or property resulting from any ideas, methods, instructions or products referred to in the content.